Monthly Notices
of the
ROYAL ASTRONOMICAL SOCIETY

MNRAS **445,** 2302–2312 (2014) doi:10.1093/mnras/stu1917

Bruck 88: a young star cluster with an old age resemblance in the outskirts of the Small Magellanic Cloud

Andrés E. Piatti[1,2]★

[1]*Observatorio Astronómico, Universidad Nacional de Córdoba, Laprida 854, 5000 Córdoba, Argentina*
[2]*Consejo Nacional de Investigaciones Científicas y Técnicas, Av. Rivadavia 1917, C1033AAJ Buenos Aires, Argentina*

Accepted 2014 September 12. Received 2014 September 8; in original form 2014 August 1

ABSTRACT

We present spectroscopic and photometric results for the Small Magellanic Cloud (SMC) cluster Bruck 88. From the comparison of the cluster integrated spectrum with template cluster spectra, we found that the Milky Way globular cluster template spectra are the ones which best resemble it. However, the extracted cluster colour–magnitude diagram reveals that Bruck 88 is a young cluster ($\log(t) = 8.1 \pm 0.1$). The derived cluster age is compatible with the presence of a bright red giant (BRG) star located ∼2.6 arcsec in the sky from the cluster centre. We serendipitously observed HW 33, a star cluster located ≈3 arcmin to the south-east from Bruck 88. We obtained for the cluster the same age than Bruck 88 and surprisingly, a BRG star located within the cluster radius also appears to be compatible with the cluster age. We estimated the MK type of the BRG star in the Bruck 88 field to be in the range G9 II/Ib–K1 III. By combining the spectrum of a star within this MK type range with a 100–150 Myr template cluster integrated spectrum, we found that a proportion 85/15 in the sense BRG/template results in a spectrum which best resembles that of Bruck 88. This result confirms that a BRG star dominates the cluster integrated spectrum, so that it causes the globular cluster appearance of its integrated light.

Key words: techniques: photometric – techniques: spectroscopic – galaxies: individual: SMC – Magellanic Clouds – galaxies: star clusters: general.

1 INTRODUCTION

The Small Magellanic Cloud (SMC) has long been known as a galaxy in which a population of genuine old star clusters does not appear to exist. Up to date, the handful of oldest SMC star clusters consists in only four objects, namely: NGC 121 (10.6 Gyr; Dolphin et al. 2001), HW 42 (9.3 Gyr; Piatti 2011), K 3 (9.0 Gyr; Da Costa & Hatzidimitriou 1998), and NGC 361 (8.1 Gyr; Mighell, Sarajedini & French 1998). The remaining small handful of relatively old clusters consists in 12 objects with ages around (6 ± 1) Gyr (Piatti et al. 2007a; Piatti 2011, 2012).

During several years, we carried out a spectroscopic campaign aiming at identifying old cluster candidates in the Large Magellanic Cloud (LMC)/SMC from their integrated spectra. Our search was based on the comparison of the observed integrated continuum energy distribution of the selected targets with the integrated spectra library of Galactic globular clusters (GGCs) built by Bica & Alloin (1986b). From this campaign two old globular LMC clusters have been identified (Dutra et al. 1999), which have been later confirmed as such (Mackey & Gilmore 2004). Another old cluster candidate was identified in the SMC, Bruck 88, for which we devote here a detailed study. As far as we are aware, this cluster has not been previously studied in detail. However, its relative position in the outskirts of the galaxy makes it also a potential old cluster candidate (see Fig. 1).

The paper is organized as follows. The integrated spectroscopic data obtained for Bruck 88 is presented in Section 2; while the cluster fundamental parameters coming from its integrated spectrum are derived in Section 3. Sections 4 and 5 deal with the photometric data and the astrophysical properties estimated for the cluster, respectively. In Section 6, we discuss the spectroscopic and photometric results, and summarize the conclusions in Section 7.

2 SPECTROSCOPIC DATA COLLECTION AND REDUCTION

The compact nature of the cluster – 0.45 arcmin in diameter (Bica et al. 2008) – makes it a good target for integrated spectroscopy. The observations were carried out at Cerro Tololo Inter-american Observatory (CTIO) through the 2003B-0447 programme (PI: A.E. Piatti) with the 1.5-m telescope during a run in 2003 September 18–21. We employed a CCD detector containing a Loral chip of 1200 × 800 pixels attached to the Cassegrain spectrograph, the

★E-mail: andres@oac.uncor.edu

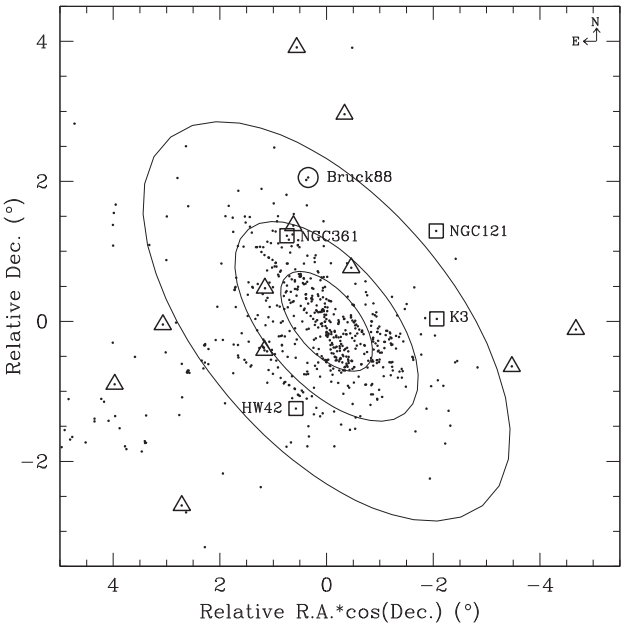

Figure 1. Spatial distribution of clusters catalogued by Bica et al. (2008) in the SMC, where the four oldest SMC clusters have been highlighted with open boxes, the relatively old clusters with open triangles, and Bruck 88 with an open circle. The cluster placed very close to Bruck 88 to the south-east is HW 33. Ellipses with semimajor axis of 1°, 2°, and 4° are overplotted.

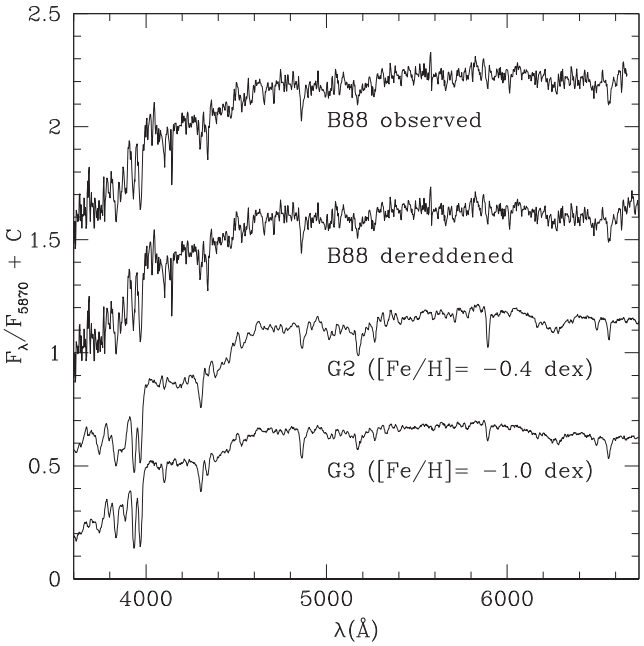

Figure 2. Observed and dereddened integrated spectra of Bruck 88 compared to the G2 and G3 template spectra.

size of each pixel being 15 μm × 15 μm; one pixel corresponds to 1.3 arcsec on the sky. The slit was set in the east–west direction and the observations were performed by scanning the slit across the objects in the north–south direction in order to get a proper sampling of cluster stars. The long slit corresponding to 7.6 arcmin on the sky allowed us to sample regions of the background sky. We used a grating of 300 lines mm^{-1}, producing an average dispersion in the observed region of ≈192 Å mm^{-1} (2.88 Å $pixel^{-1}$). The spectral coverage was ∼(3500–6800) Å. A slit width of 3.5 arcsec provided a resolution full width at half-maximum (FWHM) of ≈11.5 Å, as deduced from the comparison lamp lines. Three exposures of 15 min were taken for the cluster. The standard stars LTT 7379, LTT 7987, LTT 9239, and EG 21 (Stone & Baldwin 1983) were observed for flux calibrations. Bias, dome and twilight sky flat-fields were taken and employed for the instrumental signature calibrations.

The reduction of the spectra was carried out with the IRAF[1] package following the standard procedures. Summing up, we applied bias and flat-field corrections, performed sky subtraction, extracted and wavelength calibrated the spectra, and the rms errors involved in these calibrations are on average 0.40 Å. Finally, extinction correction and flux calibrations were applied to the cluster spectra and the three individual spectra combined.

3 SPECTROSCOPIC CLUSTER AGE AND METALLICITY

The cluster age was derived by comparing the observed spectrum to template spectra with well-determined properties, accomplished in various studies (e.g. Piatti et al. 2002b, and references therein) and made available through the CDS/Vizier catalogue data base at http://vizier.u-strasbg.fr/cgi-bin/VizieR?-source=III/219 (Santos et al. 2002). We assigned a higher weight to the overall continuum than to absorption line equivalent widths (EWs), because the latter have similar EWs for young and old clusters (Bica & Alloin 1986a,b). Note that differences between cluster and template spectra are expected to be found due to variations in the stellar composition of the cluster, such as the presence of a relatively bright star with particular spectral features or contamination of a field star close to the direction towards the cluster.

Since the continuum distribution is also affected by reddening, we first adopted a cluster colour excess of $E(B-V) = (0.03 \pm 0.01)$ mag taken from the NASA/IPAC Extragalactic Database[2] (NED).

We computed for Bruck 88 the value of the semimajor axis a parallel to the SMC main body that an ellipse would have if it were centred on the SMC centre (Crowl et al. 2001, RA = $00^h52^m45^s$, Dec. = 72° 49′ 43″ (J2000)), had a b/a ratio of 1/2 and one point of its trajectory coincided with the cluster position. We obtained $a = 3.^\circ273$. This value is larger than the mean semimajor axes of the four oldest SMC clusters ($a = (2.^\circ97 \pm 0.^\circ99)$) which are predominantly placed in the galaxy outer regions.

From the matching procedure we found that the GGC template spectra G2 ([Fe/H] = −0.4 dex) and G3 ([Fe/H] = −1.0 dex) are the ones which best resemble the dereddened cluster integrated spectrum. They resulted in lower and upper envelopes of the cluster integrated spectrum for some spectral regions with metallic bands. Fig. 2 depicts both the observed and dereddened Bruck 88 integrated spectra, as well as the G2 and G3 template spectra. All the spectra have been normalized at λ = 5870 Å and shifted by an arbitrary constant for comparison purposes.

Santos & Piatti (2004, hereafter SP04) developed a method to estimate cluster ages from visible integrated spectra. They defined S_m and S_h as the sums of the EWs of the metallic lines K (Ca II),

[1] IRAF is distributed by the National Optical Astronomy Observatories, which is operated by the Association of Universities for Research in Astronomy, Inc., under contract with the National Science Foundation.

[2] http://ned.ipac.caltech.edu/. NED is operated by the Jet Propulsion Laboratory, California Institute of Technology, under contract with the National Aeronautics and Space Administration.

Table 1. EWs (Å) of selected spectral features.

Spectrum	K(Ca II)	H(Ca II)+Hϵ	Hδ	*G* band (CH)	Hγ	Hβ	Mg I
Bruck 88	7.1 ± 0.5	8.7 ± 0.4	3.8 ± 0.5	3.3 ± 0.3	5.2 ± 0.4	3.8 ± 0.3	2.6 ± 0.3
G2	8.8 ± 0.3	7.7 ± 0.4	1.3 ± 0.1	4.4 ± 0.2	1.3 ± 0.2	3.3 ± 0.2	2.7 ± 0.1
G3	6.5 ± 0.3	6.7 ± 0.3	1.8 ± 0.1	3.6 ± 0.1	1.8 ± 0.1	3.4 ± 0.2	1.6 ± 0.1
Yf	1.9 ± 0.2	7.3 ± 0.2	7.9 ± 0.2	0.8 ± 0.2	8.3 ± 0.1	9.2 ± 0.3	0.5 ± 0.1
$0.85 \times$ Yf+$0.15 \times$ G9II	7.8 ± 0.2	8.7 ± 0.3	2.2 ± 0.1	4.6 ± 0.1	4.4 ± 0.4	3.3 ± 0.3	3.0 ± 0.2
$0.85 \times$ Yf+$0.15 \times$ K1III	7.1 ± 0.2	8.0 ± 0.3	3.2 ± 0.3	6.5 ± 0.3	3.0 ± 0.3	3.5 ± 0.2	3.2 ± 0.2

Table 2. CCD *gi* data of stars in the field of Bruck 88.

Star	RA (J2000) (h:m:s)	Dec. (J2000) ($^\circ\ '\ ''$)	g (mag)	$\sigma(g)$ (mag)	$g-i$ (mag)	$\sigma(g-i)$ (mag)	n
–	–	–	–	–	–	–	–
20	00:57:18.373	−70:49:07.82	22.029	0.013	2.216	0.014	8
21	00:57:18.828	−70:49:07.36	19.943	0.005	0.368	0.007	8
22	00:56:48.942	−70:49:07.23	21.428	0.006	0.684	0.012	8
–	–	–	–	–	–	–	–

G band (CH), and Mg I, and of the Balmer lines Hδ, Hγ, and Hβ, respectively. As they shown, S_m and S_h prove to be useful in the discrimination of old, intermediate-age, and young systems. Also, SP04 defined diagnostic diagrams (DDs) involving S_h and S_m with a view to discriminating cluster ages for systems younger than 10 Gyr and metallicities for systems older than 10 Gyr.

We first defined the continuum in the spectrum of Bruck 88 according to the criteria outlined by Bica & Alloin (1986b) and then we measured EWs within their selected spectral windows, using IRAF task SPLOT. The boundaries of the spectral windows and their principal absorbers are indicated in Bica & Alloin (1986b). The resulting EW measurements (Å) are shown in Table 1 where the errors come from tracing slightly different continua. Then, by using the DDs we found that S_m and S_h fall in the region of old clusters ([Fe/H] ≤ -1.4 dex). On the other hand, if we compared the individual EWs listed in Table 1 for Bruck 88 with those for the G2, G3, and Yf (see Section 6) templates, we would conclude from K (Ca II), *G* band, Hβ and Mg I that Bruck 88 is an old cluster, from Hδ and Hγ that it is an intermediate-age cluster, and from H (Ca II)+Hϵ that the cluster could either be old or young ($\sim$100 Myr). The difference between K (Ca II) and H (Ca II)+Hϵ features in old and young objects is a well-known behaviour studied by Rose (1984, 1985). Nevertheless, the suggested age points to the need of a high-quality cluster colour–magnitude diagram (CMD), where its red giant branch (RGB), red clump (RC), main-sequence turnoff and fainter main-sequence (MS) stars can be clearly distinguished.

4 SDSS *g*, *i* PHOTOMETRY

In order to confirm whether Bruck 88 belongs to the group of the oldest known clusters in the SMC, we built the cluster CMD from *g* and *i* images obtained with the Gemini South telescope and the GMOS-S instrument (scale = 0.146 arcsec per (2 × 2 binned) pixel) in the night of 2014 January 5. The detector is a 3 × 1 mosaic of 2k × 4k EEV CCDs, yielding a field of view (FOV) of $\sim$5.5 arcmin × 5.5 arcmin. We obtained 4 × (30 (short) + 280 (long)) sec exposures with the *g* and *i* filters, respectively, through programme GS-2013B-60 (PI: Piatti). The data were obtained with an excellent seeing (0.48 arcsec–0.70 arcsec FWHM), under photometric conditions, and with airmass between 1.41 and 1.51.

The data reduction followed the procedures documented in the Gemini Observatory webpage[3] and utilized the GEMINI/GMOS package in IRAF. We performed overscan, trimming, bias subtraction, flattened all data images, etc. Observations of photometric standard stars (E5_b and GD_108 standard fields) chosen from the standard star catalogue calibrated directly in the SDSS system (http://www-star.fnal.gov) were included in the baseline calibrations for GMOS. The relationships between instrumental and standard magnitudes, fitted with the FITPARAMS IRAF routine, resulted to be

$$g = -3.366 \pm 0.012 + g_{\rm std} + (0.080 \pm 0.010) \times X_g - (0.011 \pm 0.013) \times (g-i)_{\rm std}\ ({\rm rms} = 0.035) \quad (1)$$

$$i = -2.937 \pm 0.016 + i_{\rm std} + (0.018 \pm 0.010) \times X_i + (0.013 \pm 0.018) \times (g-i)_{\rm std}\ ({\rm rms} = 0.038), \quad (2)$$

where X represents the effective airmass.

Bruck 88 photometry was performed using the star-finding and point spread function (PSF) fitting routines in the DAOPHOT/ALLSTAR suite of programs (Stetson, Davis & Crabtree 1990). We derived a quadratically varying PSF per image by fitting $\sim$60 least contaminated stars. We then used the ALLSTAR program to apply the resulting PSF to the identified stellar objects Only objects with $\chi < 2$, photometric error less than 2σ above the mean error at a given magnitude, and |SHARP| < 0.5 were kept in each filter, and then the remaining objects in the *g* and *i* lists were matched with a tolerance of 1 pixel and raw photometry obtained. The gathered photometric information was standardized using equations (1) and (2). Table 2 provides this information: a running number per star, equatorial coordinates, the averaged *g* magnitudes, and $g-i$ colours, their respective rms errors $\sigma(g)$ and $\sigma(g-i)$, and the number of observations per star. Only a portion of it is shown here for guidance regarding its form and content. The whole content of Table 2 is available in the online version of the journal in Oxford journals, at http://access.oxfordjournals.org.

[3] http://www.gemini.edu

5 ANALYSIS OF THE CMD

In Fig. 3, we show the CMD of stars measured in the field of Bruck 88 with errors in g and $g - i$ smaller than 0.1 mag. The behaviour of $\sigma(g)$ and $\sigma(g - i)$ is represented by error bars in the right-hand side of the figure. As can be seen, the most obvious traits are the long MS which extends over a range of approximately 8 mag in g, a populous subgiant branch (SGB), an RC and an RGB. The RC is not tilted so that differential reddening can be assumed to be negligible along the line of sight.

In order to obtain a circular extracted CMD where the fiducial features of the cluster are clearly seen, we used the coordinates of the cluster centre and its radius given by Bica et al. (2008). Fig. 4 shows the resulting extracted CMD with all the stars measured within the cluster circle, which reveals that Bruck 88 is a young cluster, although some contamination from field stars is unavoidable particularly at the fainter magnitude regime. This result is opposite to that found from the cluster integrated spectrum, and makes us to wonder about the origin from which a young (blue MS) cluster appears much older (redder) to its integrated light. We discard the possibility of field SGB–RC–RGB stars contamination in the cluster integrated spectrum, since the extracted CMD (see Fig. 4) was built from stars distributed throughout an area that covers a sky region similar to that surveyed from integrated spectroscopy. We rather think that we are dealing with a case of stochastic effects caused by the presence of a bright red giant (BRG; $g = 16.301 \pm 0.011$, $g - i = 1.120 \pm 0.011$) star placed somewhere along the cluster line of sight. This BRG is ≈2.6 arcsec in the sky from the cluster centre.

In order to derive the cluster age through the matching of theoretical ischrones to its CMD, we assumed a distance modulus equal to that of the SMC ($(m - M)_o = 18.90 \pm 0.10$ ($60.0^{+3.0}_{-2.5}$ kpc, Glatt, Grebel & Koch 2010)), the present-day galaxy metallicity (−0.7 dex; Piatti & Geisler 2013) – given the apparent youth of the cluster – and the reddening adopted in Section 3, $E(B - V) = 0.03$ mag.

We took advantage of theoretical isochrones computed with core overshooting for the SDSS photometric system (Bressan et al. 2012) to estimate the cluster age. In the matching procedure with a naked eye, we adopted the cluster age as the age of the isochrone which best reproduced the cluster's MS ($\log(t) = 8.1 \pm 0.1$). We found that isochrones bracketing the derived mean age by $\Delta(\log(t/\mathrm{yr})) = \pm 0.1$ reasonably represent the overall age uncertainty. Note that the derived cluster age is compatible with the presence of the BRG star mentioned above within the cluster stellar population. Fig. 4 illustrates the result of the isochrone matching procedure.

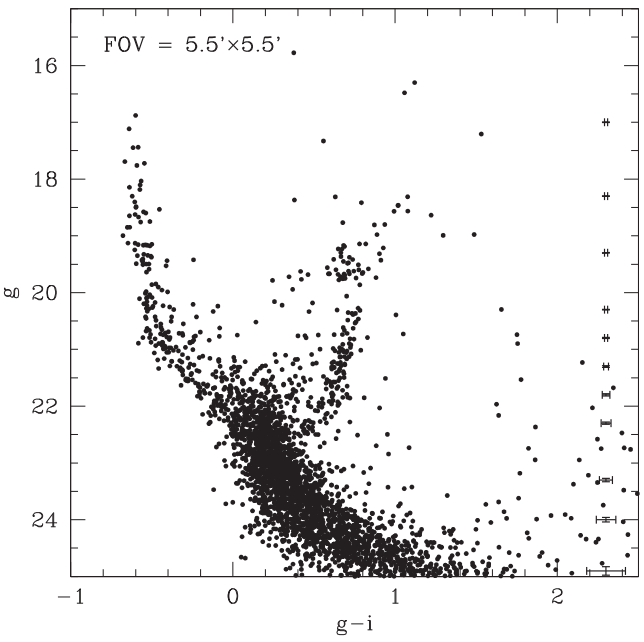

Figure 3. CMD of the stars measured in the field of Bruck 88.

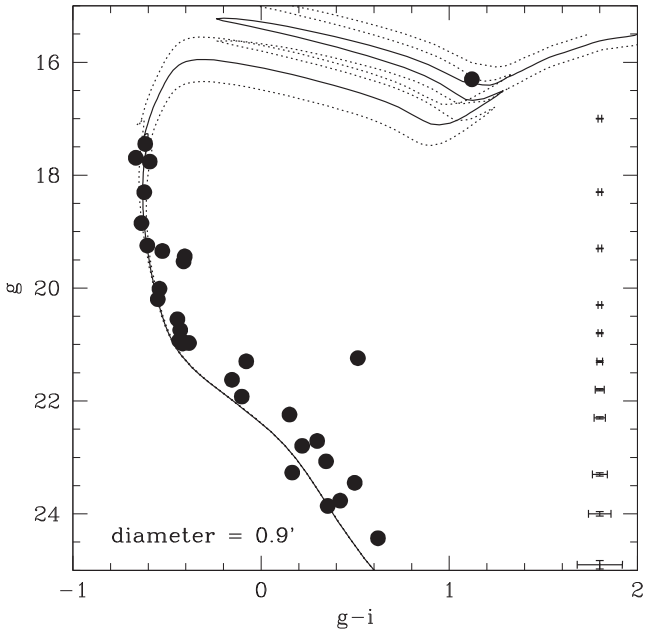

Figure 4. Bruck 88's CMD built using stars distributed within the cluster circle. Theoretical isochrones from Bressan et al. (2012) for $\log(t) = 8.0$, 8.1, and 8.2, and metallicity [Fe/H] = −0.7 dex are superimposed.

We serendipitously observed HW 33 within the GMOS-S FOV, a star cluster located ≈3 arcmin (52.3 pc) to the south-east from Bruck 88. We followed the same procedure of extracting stars around the cluster centre and within the cluster radius and of building the cluster CMD. We obtained a cluster reddening of $E(B - V) = (0.03 \pm 0.01)$ mag from the NED. From the matching of theoretical isochrones ([Fe/H] = −0.7 dex) HW 33 turns out to be of the same age as Bruck 88 ($\log(t) = 8.1 \pm 0.1$, see Fig. 5) and surprisingly, a BRG star ($g = 16.481 \pm 0.004$, $g - i = 1.058 \pm 0.004$) located within the cluster radius, also appears to be compatible with the cluster age.

6 DISCUSSION

In this section, we describe a possible explanation aiming at making compatible the results coming from the photometric data and our knowledge of the cluster from its integrated spectrum. We propose that the observed cluster integrated spectrum is the result of the combination of a template spectrum for an ∼100 Myr old cluster and the spectrum of a bright giant star. Furthermore, we support the possibility that the Bruck 88's integrated spectrum is dominated by the light of a bright giant star which mimics the integrated light of an old stellar aggregate. Indeed, when summing to the cluster integrated magnitude (computed from all stars in Fig. 4 with $g > 17$ mag) the magnitude of the BRG star, Bruck 88 becomes 1.6 and 4.0 times brighter in g and i, respectively. In order to confirm such a possibility, we first obtained the MK type of the aforementioned BRG star, then we selected a spectrum for that MK type from the stellar spectra library built by Jacoby, Hunter &

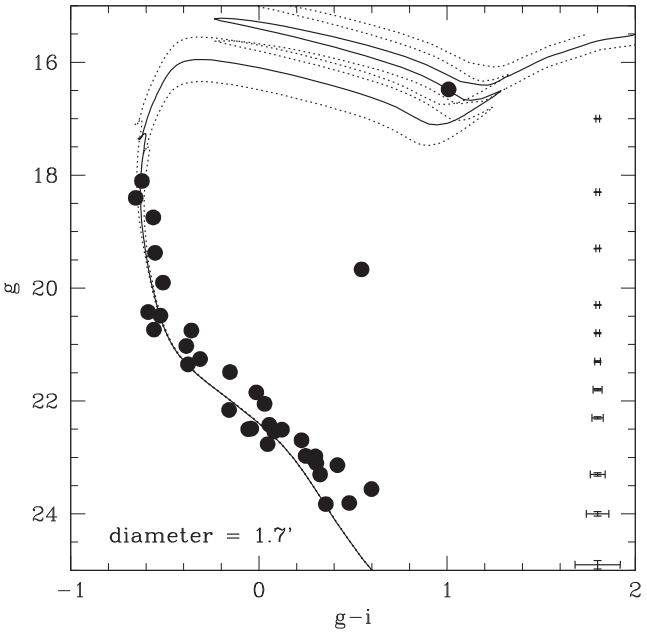

Figure 5. Same as Fig. 4 for HW 33.

Christian (1984), and finally we combined it with an integrated template spectrum for a 100 Myr old cluster taken from Santos et al. (2002).

For the MK type of the BRG star, we interpolated Schmidt-Kaler (1982)'s MK type versus $(B-V)_o$ and MK type versusM_V relations from the computed intrinsic colours $(B-V)_o$ and visual absolute magnitudes M_V of the BRG star. We computed M_V by combining the SMC distance modulus $(m-M)_o = 18.9$, the cluster reddening $E(B-V) = 0.03$, the visual to selective absorption ratio $R = A_V/E(B-V) = 3.1$, and the relation for $g-V$ given by Jordi, Grebel & Ammon (2006) through the expression:

$$M_V = 0.124 + g - 0.630 \times (B-V)_o - R \times E(B-V) - (m-M)_o, \quad (3)$$

and the intrinsic $(B-V)_o$ colour by combining the relationships between $(B-V)_o$ and $(V-I)_o$ of Caldwell et al. (1993, see fig. 26) and that between $(V-I)_o$ and $(g-i)_o$ of Jordi et al. (2006) given by

$$(g-i)_o = 1.481 \times (V-I)_o - 0.536. \quad (4)$$

We obtained $M_V = (-3.28 \pm 0.20)$ mag and $(B-V)_o = (1.10 \pm 0.02)$ mag, which lead to an MK type of G9/K0 II/Ib for the BRG star.

If the RGB star were not located at the SMC distance but somewhere in front of it, then it should be mainly moved in the HR diagram along a vertical line from LC II towards LC III region, because of the low reddening along the line of sight ($E(B-V) = 0.03$). In case it were a LC III star, its $(B-V)_o$ colour would correspond to a K1 MK type star (Schmidt-Kaler 1982) and its M_V would be 0.6 mag, which corresponds to a distance of 10.2–10.5 kpc (see equation 3), depending on whether the $E(B-V)$ is assumed to be 0.00 or 0.03 mag.

Bearing in mind the possible MK types of the BRG star, we selected spectra of stars with MK types in the range G9 II/I–K1 III, namely: SAO 55164 (K0 III), SAO 77849 (K2 III), HD 249384 (G8 II), HD 250368 (G9 II), HD 187299 (G5 I), and HD 186293 (K0 I) from Jacoby et al. (1984)'s library. We normalized all spectra at $\lambda = 5870$ Å in order to compare them to those from the cluster integrated spectra library. We found that all selected spectra are tightly similar to each other with small difference in some metallic bands. When individually combining them with the template cluster integrated spectrum Yf (100–150 Myr; Santos et al. 2002), we found that a proportion 85/15 in the sense BRG/template (BRG + template = 100) results in a spectrum which best resembles that of Bruck 88. Figs 6 and 7 illustrate the combination process and the resulting comparison with Bruck 88's integrated spectrum. On the other hand, EWs of some selected spectral features for these spectra combinations (see Table 1) seem to be more similar to those of

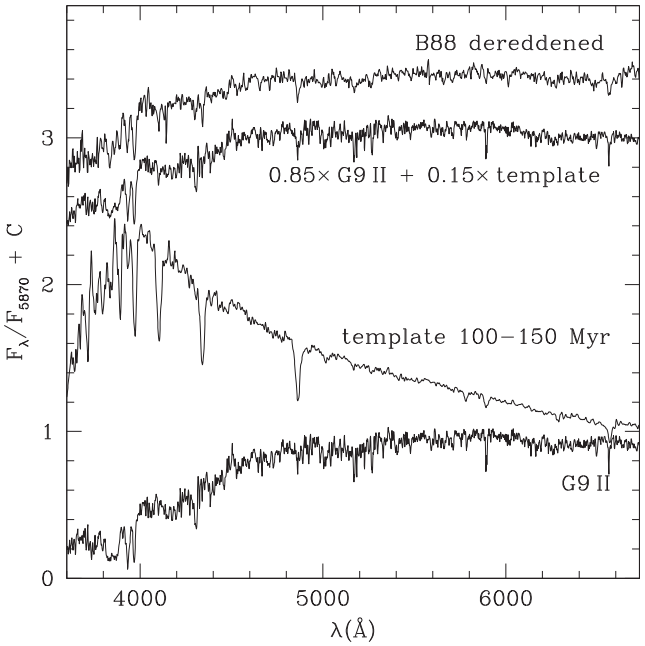

Figure 6. Dereddened integrated spectra of Bruck 88 compared to that resulting from the combination of the template 100–150 Myr integrated spectrum and of a G9 II MK type star spectrum.

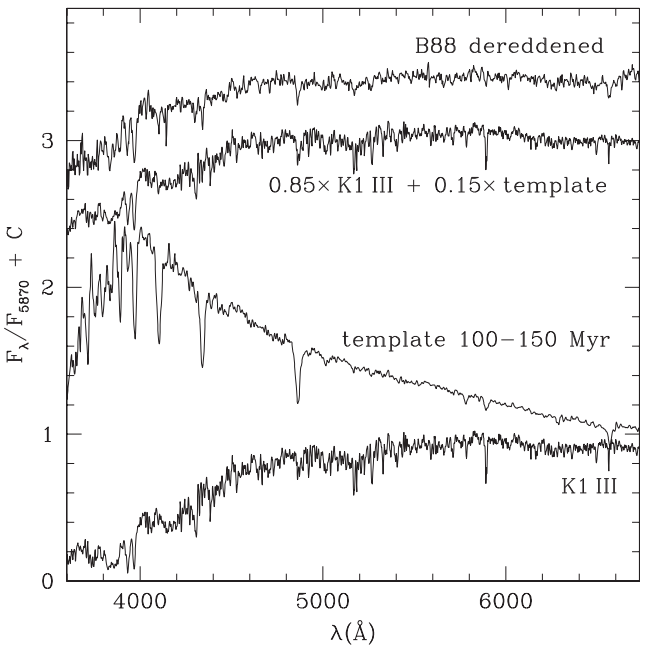

Figure 7. Same as Fig. 6 for a K1 III MK type star spectrum.

Bruck 88 than of G2, G3, and Yf, respectively. This result confirms that a RGB star dominates the cluster integrated spectrum, so that it causes the globular cluster appearance of its integrated light (see Fig. 2).

7 SCOPE OF THE INTEGRATED SPECTROSCOPY

The misleading integrated spectrum of Bruck 88 drove us to investigate whether a similar situation might exist for other clusters in the literature. Furthermore, we took advantage of such a study to assess the level of accuracy and reliability of age estimates derived from the template matching technique applied in Section 3. We embarked in such an analysis by first searching the available literature for studies about star clusters based on integrated spectroscopy. Particularly, we focused on those works that made use of the template integrated spectra library employed here (Santos et al. 2002). We found a total of 230 clusters with published ages obtained from this technique. Table 3 lists the entire cluster sample along with the age estimates ($\log(age)_{spec}$) and the respective references.

From Table 3, we secondly searched the literature for cluster age estimates derived from the analysis of CMDs, which provide ages with uncertainties typically of $\sigma(\log(age)) \sim 0.1$ (see e.g. Piatti 2010, 2014; Maia, Piatti & Santos 2014). We found 198 clusters which fulfilled our request, and their age values and the corresponding references have also been included in Table 3 ($\log(age)_{cmd}$). As far as we are aware, this cluster sample largely supersedes those previously used to set the performance of the integrated spectroscopy in estimating cluster ages from the comparison with ages derived from other methods (see e.g. Asa'd, Hanson & Ahumada 2013). We note that two objects have been recently classified as cluster remnants, while 11 other objects have been found not to be real physical systems from detailed CMD analyses. All of them have been labelled with the word 'remnant' or 'non-cluster' in Table 3. This flub from the integrated spectroscopy side comes from the fact that the technique is not able to size up whether it deals with the presence of a genuine star cluster, or with a chance grouping of stars or with the effect of a non-uniform distribution of the interstellar material along the line of sight.

The gathered information in Table 3 was then plotted in Fig. 8, which depicts the relationship between both different age estimates. We have drawn the identity relation with a black line, and those shifted by ± 0.1, and ± 0.3 with dark grey and clear grey lines, respectively. Clusters whose age estimates differ ($|\log(age)_{spect} - \log(age)_{cmd}|$) in 0.1, between 0.1 and 0.3, 0.3 and 0.35, and more than 0.4 have been plotted with open, filled clear grey, dark grey, and black circles, respectively. Bruck 88 has been represented by a bigger open partially filled circle. As can be seen, the relationship is far from being reasonably tight but highly scattered. Indeed, Fig. 9 shows the distribution of clusters in terms of their age differences (absolute values) using the same coloured-grey-scale as in Fig. 8. The age differences larger than 0.4 (black filled squares) represent ~55 per cent of the cluster sample. This result suggests that the integrated spectroscopy matching technique should be used with caution, since it particularly might misguide when applying it in studies of stellar population synthesis in galaxies (Ahumada, Clariá & Bica 2007; Palma et al. 2008a; Talavera et al. 2010; Asa'd et al. 2013; Minniti et al. 2014).

Fig. 8 also suggests that the cluster sample is not homogeneously distributed in age; a trend that is quantitatively confirmed by Fig. 10. Thus, in order to produce a more realistic picture of the integrated spectroscopy performance, we computed the mean, the median, the standard deviation, and the mean error of the median as a function of the cluster age. The mean error of the median is more representative of the actual dispersion of the age differences, since it takes into account the number of clusters used to compute the mean and median ages. Similarly, the median is more appropriate to consider in our analysis, because of the distribution of clusters in the $|\log(age)_{spect} - \log(age)_{cmd}|$ versus $\log(age)_{cmd}$ plane for each age interval is far from being a normal distribution. In general, the mean values of the age difference (absolute value) resulted much larger than the median ones, which would lead to draw less favourable conclusions for the integrated spectroscopy template matching technique, if we used them for assessing its accuracy and reliability. For this reason, we show in Fig. 11 the behaviour of the resulting median values of the age difference and their respective mean errors. As can be seen, a mean discrepancy of ~0.4 in log(age) dominates the integrated spectroscopy age estimates respect to the literature values. The differences are reasonably good (~0.1–0.2) for a couple of age intervals. However, they come out from a relatively small statistical cluster sample and the respective mean errors are considerably large, except in the case of oldest clusters. Moreover, Fig. 11 shows that age intervals with 2–3 times more clusters ($\log(age)_{cmd} \sim 7.8$–8.2) do not account for age differences smaller than ~0.3. Likewise, there are some age intervals with particularly much larger age differences ($\log(age)_{cmd} \sim 6.8$–7.2, 8.6–8.8, and 9.2–9.6).

These results point to the need of entering some caveats in the use of the integrated spectroscopy matching technique to estimate cluster ages as it has been applied until the present. On the one hand, the integrated spectra library is constrained to certain age ranges, which implies that only ages associated with the available template spectra can be assigned to any integrated spectrum under study. In order to enlarge and improve the sample of template spectra, it is required to obtain integrated spectra of clusters with well-known fundamental parameters. However, several works that have used such a technique (see Table 3) mentioned that integrated spectra of clusters whose ages were estimated from the integrated spectra matching procedure were used to define new template spectra or to improve existing ones. This approach suffers from internal inconsistency and makes any attempt of enlarging the integrated spectra library to fall apart. On the other hand, integrated spectra are often affected at different levels by the contamination of field stars. This is an issue that unfortunately the integrated spectroscopy cannot handle, particularly in relatively crowded fields or in low surface brightness objects. Finally, the presence of evolved or peculiar relatively bright stars within the cluster population can also lead to a disguised appearance of the cluster integrated light. For instance, we found that Pismis 7 and Ruprecht 107, among others, have red supergiant stars which make the clusters appear older than they are (see Table 3), similarly as it happens with the integrated spectrum of Bruck 88. We think that these aspects or a combination of them can explain the discrepancies shown in Fig. 11. Nevertheless, we foresee that these kind of constraints will be partially solved with the advent of synthetic integrated spectra. It is a promising field to exploit that deserve much more development, although the assumption of a particular cluster composite stellar population to combine different synthetic spectra is unavoidable.

8 CONCLUSIONS

During several years we carried out a spectroscopic campaign aiming at identifying old cluster candidates in the L/SMC from their integrated spectra. From that campaign we identified Bruck 88,

Table 3. Age estimates derived from CMDs and integrated spectra.

Cluster	$\log(age)_{spec}$	Ref.	$\log(age)_{cmd}$	Ref.	Cluster	$\log(age)_{spec}$	Ref.	$\log(age)_{cmd}$	Ref.
Alessi 14	8.7	10	Non-cluster	11	NGC 1856	8.45	1	8.45	2
Alessi 15	9.0	10	9.25	11	NGC 1859	8.70	9	8.1	3
Alessi 16	9.50	10	9.05	11	NGC 1863	6.90	1	7.7	4
Basel 18	7.7	31	7.6	11	NGC 1870	7.7	59	7.5	58
Berkeley 75	9.3	38	9.5	50	NGC 1887	7.8	22	8.1	3
Berkeley 77	9.55	30	8.8	15	NGC 1894	8.1	59	7.75	58
Berkeley 80	8.8	31	8.6	51	NGC 1897	8.65	43	–	–
BH 55	8.8	14	9.05	11	NGC 1902	7.8	59	8.0	3
BH 58	8.6	14	–	–	NGC 1903	7.8	1	–	–
BH 72	8.7	10	9.1	11	NGC 1905	8.5	43	–	–
BH 80	6.65	38	6.7	11	NGC 1913	7.8	59	7.50	58
BH 87	8.0	38	8.4	11	NGC 1920	6.7	9	–	–
BH 90	8.55	14	7.95	11	NGC 1932	8.6	59	8.1	3
BH 92	8.55	14	7.6	11	NGC 1940	7.8	59	8.0	3
BH 121	6.6	14	6.65	53	NGC 1943	8.45	63	7.50	58
BH 132	8.0	38	–	–	NGC 1944	7.8	22	–	–
BH 151	6.45	31	–	–	NGC 1971	7.7	59	7.8	58
BH 202	9.0	24	8.05	11	NGC 1972	7.85	22	7.6	58
BH 205	7.0	14	7.1	11	NGC 1983	6.65	1	7.45	44
BH 217	7.55	14	7.65	11	NGC 1984	6.65	1	7.8	3
Bochum 2	6.7	31	6.7	52	NGC 1986	7.8	22	–	–
Bochum 12	7.5	38	7.6	11	NGC 1994	6.50	1	7.7	3
Bochum 14	6.45	34	7.0	11	NGC 2000	7.6	22	8.0	3
Bruck 50	6.6	26	7.0	27	NGC 2002	6.65	1	7.1	3
Collinder 258	8.0	14	8.05	53	NGC 2011	6.65	1	7.4	3
Dolidze 34	8.8	31	–	–	NGC 2031	7.80	1	8.2	5
ESO 065-SC07	9.4	14	9.1	11	NGC 2038	7.8	59	–	–
ESO 211-SC09	9.55	10	9.05	11	NGC 2053	7.85	22	8.25	3
ESO 260-SC06	9.50	10	8.80	11	NGC 2065	7.8	1	–	–
ESO 277-SC04	9.0	10	–	–	NGC 2095	7.6	9	7.9	3
ESO 313-SC03	9.50	10	8.85	11	NGC 2097	8.9	23	–	–
ESO 315-SC14	8.70	10	7.85	11	NGC 2118	7.8	59	7.2	3
ESO 324-SC15	9.00	30	Remnant	16	NGC 2130	7.8	59	7.9	3
ESO 332-SC11	6.85	10	–	–	NGC 2135	7.7	59	7.5	58
ESO 371-SC25	7.00	10	9.55	11	NGC 2136	7.8	23	7.3	3
ESO 429-SC02	6.85	31	8.6	11	NGC 2137	9.0	22	8.1	3
ESO 429-SC13	8.0	14	–	–	NGC 2140	7.8	22	8.0	3
ESO 445-SC74	9.45	31	8.2	11	NGC 2155	9.00	1	9.55	6
ESO 492-SC02	6.90	14	Non-cluster	11	NGC 2156	6.90	1	7.9	3
ESO 502-SC19	9.00	10	Remnant	13	NGC 2157	7.80	1	7.2	3
Haffner 7	8	38	9.2	40	NGC 2164	6.9	1	7.3	3
Hodge 9	8.9	23	–	–	NGC 2166	8.5	43	–	–
Hogg 3	7.9	38	Non-cluster	39	NGC 2172	6.90	30	7.9	3
Hogg 9	8.45	31	7.45	11	NGC 2173	6.90	1	9.3	7
Hogg 10	7.5	31	7.0	33	NGC 2181	8.6	43	–	–
Hogg 11	8.5	38	7.1	11	NGC 2197	8.6	43	–	–
Hogg 12	7.9	38	7.5	42	NGC 2213	8.70	1	9.25	7
Hogg 14	8.45	24	8.1	11	NGC 2249	8.45	1	9.15	7
Hogg 15	6.65	14	7.3	18	NGC 2311	8.45	31	8.0	32
Hogg 22	6.65	31	6.8	11	NGC 2368	7.7	38	non cluster	39
HS 109	7.65	22	8.0	3	NGC 2409	7.7	31	–	–
HW 8	7.7	61	8.0	3	NGC 2459	9.0	10	non cluster	11
HW 73	7.7	35	8.1	69	NGC 2587	9.0	14	8.7	56
HW 85	7.2	26	9.35	29	NGC 2635	9.2	38	8.8	11
IC 1611	8.1	60	8.2	3	NGC 3255	8.45	24	8.3	11
IC 1624	7.75	35	8.3	27	NGC 3590	7.6	24	7.5	42
IC 1626	8.45	60	8.35	3	NGC 4439	7.6	24	7.9	11
IC 1641	8.5	61	8.3	3	NGC 4463	7.5	24	7.5	11
Kron 3	9.85	61	9.95	65	NGC 4609	8.1	24	7.7	25
Kron 5	8.9	61	9.3	64	NGC 5168	8.1	24	8.0	11
Kron 6	9.3	61	9.1	62	NGC 5281	7.5	31	7.15	11
Kron 7	9.6	61	9.55	65	NGC 5606	6.65	38	7.1	11
Kron 28	9.0	61	9.3	6	NGC 6204	7.8	31	7.9	11

Table 3 – *continued*

Cluster	log(age)$_{spec}$	Ref.	log(age)$_{cmd}$	Ref.	Cluster	log(age)$_{spec}$	Ref.	log(age)$_{cmd}$	Ref.
Kron 34	8.45	26	8.6	27	NGC 6268	7.8	14	7.6	11
Kron 42	7.65	61	7.8	3	NGC 6604	6.5	31	6.8	11
Lindsay 5	8.9	61	9.6	64	Pismis 7	9.65	31	8.7	11
Lindsay 28	9.0	35	9.0	29	Pismis 17	9.5	38	7.0	11
Lindsay 39	7.2	61	8.0	3	Pismis 20	6.7	31	6.9	11
Lindsay 51	7.2	61	7.8	3	Pismis 21	7.90	14	Non cluster	19
Lindsay 56	6.7	35	7.4	27	Pismis 23	8.5	14	8.5	11
Lindsay 66	7.2	61	7.4	3	Pismis 24	6.7	31	7.0	11
Lindsay 95	7.8	26	8.4	28	Ruprecht 2	9.55	31	–	–
Lindsay 114	9.75	35	8.15	36	Ruprecht 14	9.6	10	–	–
Lyngå 1	8.0	31	8.0	11	Ruprecht 17	8.7	10	–	–
Lyngå 4	9.0	10	9.1	11	Ruprecht 38	9.0	10	–	–
Lyngå 11	8.65	14	8.8	54	Ruprecht 107	9.55	24	7.5	11
Markarian 38	7.0	31	6.75	55	Ruprecht 144	8.00	17,38	8.65	20
Melotte 105	8.0	70	8.55	19	Ruprecht 150	9.00	10	Non cluster	12
NGC 121	10.1	35	10.0	46	Ruprecht 158	8.85	14	Non cluster	21
NGC 241	7.45	35	8.35	37	Ruprecht 159	9.3	14	–	–
NGC 242	7.2	35	7.8	37	Ruprecht 164	8.9	14	9.0	11
NGC 256	7.4	35	7.8	3	Sher 1	7.5	24	6.7	11
NGC 265	7.75	35	8.35	3	SL 14	7.2	22	8.3	3
NGC 269	8.8	61	8.5	27	SL 56	8.1	23	7.5	3
NGC 290	7.4	35	7.6	3	SL 58	7.8	22	8.0	3
NGC 294	8.5	61	8.45	3	SL 76	7.7	22	8.1	3
NGC 306	6.85	35	7.7	3	SL 79	8.0	22	8.3	3
NGC 330	7.6	45	7.4	3	SL 106	8.15	8	7.7	3
NGC 411	9.0	61	9.2	65	SL 116	7.7	23	7.8	3
NGC 416	9.75	35	9.85	41	SL 152	8.1	23	8.6	3
NGC 419	8.9	61	9.1	65	SL 168	7.65	22	8.3	3
NGC 422	8.5	61	8.15	3	SL 234	6.6	22	7.95	3
NGC 458	7.7	61	8.2	6	SL 237	7.8	45	7.3	3
NGC 643	9.0	35	9.05	29	SL 242	7.55	60	7.9	3
NGC 796	6.7	35	8.05	36	SL 255	7.8	22	7.8	3
NGC 1611	8.1	26	Non-cluster	49	SL 256	7.8	8	7.8	3
NGC 1626	8.45	26	Non-cluster	11	SL 360	6.65	22	–	–
NGC 1651	8.45	1	9.3	2	SL 364	7.6	22	8.0	3
NGC 1695	8.2	9	8.0	3	SL 386	7.8	22	8.1	3
NGC 1696	8.65	43	–	–	SL 410	8.45	8	8.05	3
NGC 1698	7.8	9	8.0	3	SL 425	9.00	8	8.2	3
NGC 1702	8.1	9	7.8	3	SL 463	7.7	22	7.7	3
NGC 1704	8.45	9	7.5	3	SL 477	7.7	22	7.9	3
NGC 1711	6.50	1	7.2	3	SL 508	7.8	59	–	–
NGC 1732	7.8	22	7.7	3	SL 543	8.45	8	7.9	3
NGC 1754	10.1	45	10.2	47	SL 551	7.2	22	7.9	3
NGC 1775	7.8	23	7.85	58	SL 566	7.8	22	7.85	58
NGC 1793	7.8	9	8.0	3	SL 624	8.7	8	–	–
NGC 1804	7.7	59	7.8	3	SL 709	8.1	59	7.1	3
NGC 1815	8.1	9	7.8	3	SL 763	7.8	22	8.0	3
NGC 1822	8.1	22	8.0	3	Trumpler 15	6.5	34	6.9	11
NGC 1828	7.7	23	–	–	Trumpler 21	7.5	31	7.7	11
NGC 1836	8.45	45	8.6	48	Trumpler 27	6.5	14	Non cluster	57
NGC 1839	8.4	45	8.1	4	WG 1	6.85	26	–	–
NGC 1850	6.90	1	7.3	3	–	–	–	–	–

Note: Ref. (1) Asa'd et al. (2013), (2) Kerber, Santiago & Brocato (2007), (3) Glatt et al. (2010), (4) Piatti et al. (2003a), (5) Mucciarelli et al. (2006), (6) Piatti et al. (2002a), (7) Piatti et al. (2014), (8) Oddone et al. (2012), (9) Minniti et al. (2012), (10) Benítez-Llambay et al. (2010), (11) Dias et al. (2002), (12) Vázquez et al. (2008), (13) Bica et al. (2001), (14) Ahumada, Clariá & Bica (2009), (15) Lata et al. (2010), (16) Pavani et al. (2011), (17) Ahumada et al. (2000), (18) Piatti et al. (2002c), (19) Piatti & Clariá (2001), (20) Camargo, Bonatto & Bica (2009), (21) Vázquez et al. (2010), (22) Talavera et al. (2009), (23) Palma et al. (2008a), (24) Ahumada et al. (2008), (25) Kook, Sung & Bessell (2010), (26) Talavera et al. (2010), (27) Chiosi et al. (2006), (28) Piatti et al. (in preparation), (29) Piatti et al. (2011b), (30) Palma et al. (2008b), (31) Ahumada et al. (2007), (32) Piatti, Clariá & Ahumada (2010b), (33) Delgado, Alfaro & Yun (2011), (34) Ahumada et al. (2006), (35) Ahumada et al. (2002), (36) Piatti et al. (2007b), (37) Maia et al. (2014), (38) Ahumada et al. (2001), (39) Piatti, Clariá & Ahumada (2011a), (40) Carraro, Beletsky & Marconi (2013), (41) Schuster et al. (2006), (42) Piatti, Clariá & Ahumada (2010a), (43) Minniti et al. (2014), (44) Gouliermis et al. (2010), (45) Ahumada et al. (2011), (46) Dolphin et al. (2001), (47) Olsen et al. (1998), (48) Piatti et al. (2003b), (49) Jones et al. (2009), (50) Carraro et al. (2005), (51) Tapia et al. (2010), (52) Moitinho et al. (2006), (53) Kharchenko et al. (2005), (54) Piatti, Clariá & Ahumada (2006), (55) Santos-Silva & Gregorio-Hetem (2012), (56) Piatti, Clariá & Ahumada (2009), (57) Perren, Vázquez & Carraro (2012), (58) Dieball, Müller & Grebel (2002), (59) Clariá et al. (2007), (60) Talavera et al. (2007), (61) Piatti et al. (200b5), (62) Matteucci et al. (2002), (63) Santos et al. (2006), (64) Piatti et al. (2005a), (65) Da Costa & Hatzidimitriou (1998).

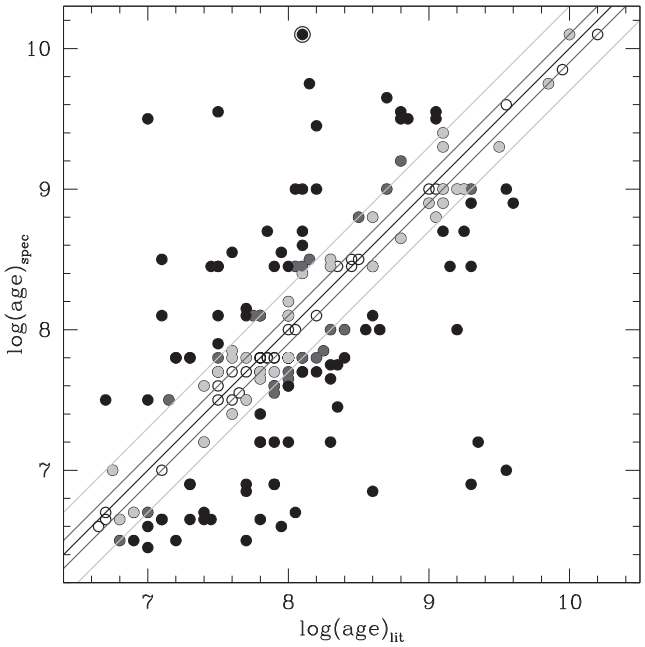

Figure 8. Comparison of age estimates derived from the matching of integrated spectra with those from the literature.

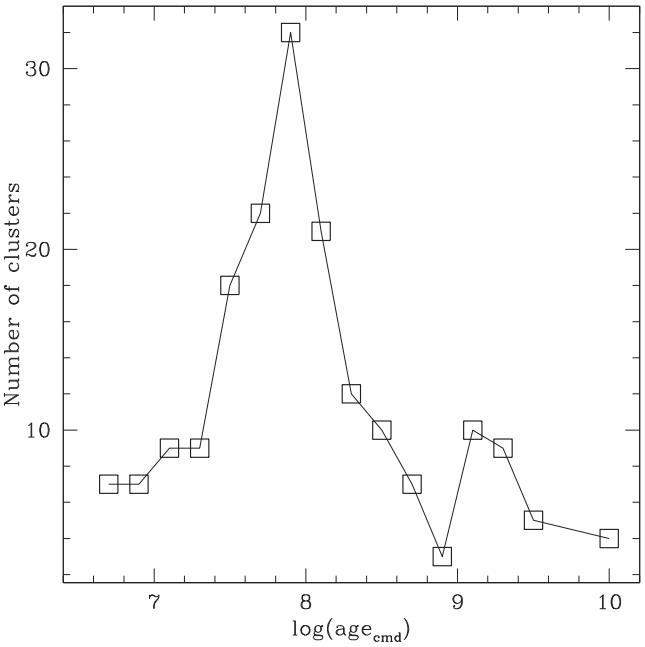

Figure 10. Distribution of clusters of Table 3 as a function of age (CMD values).

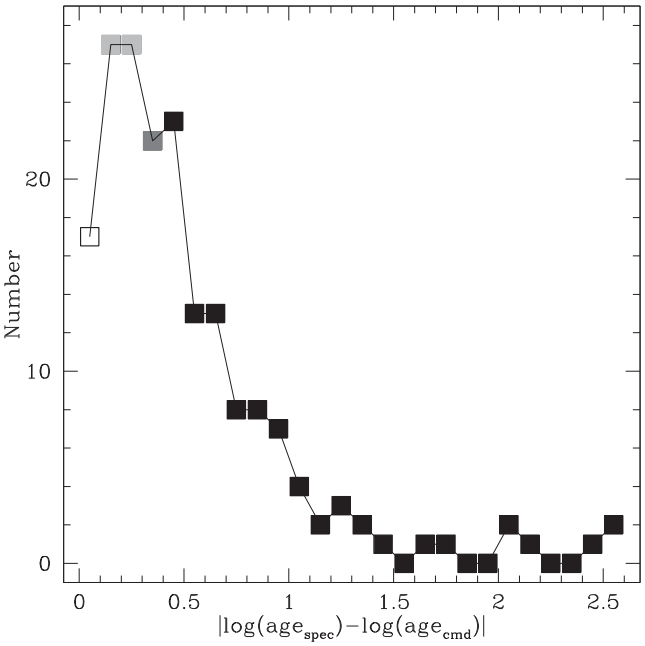

Figure 9. Distribution of the difference between ages derived from the matching of integrated spectra and those from CMDs (absolute values).

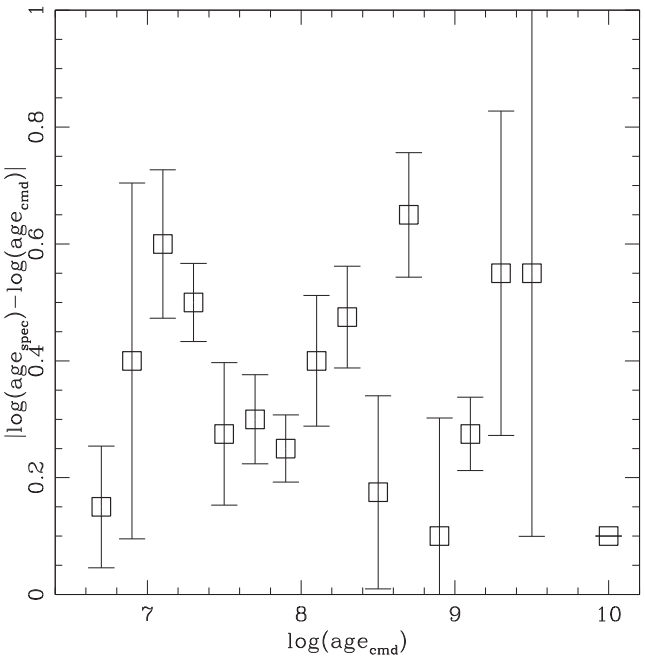

Figure 11. Age difference (absolute value) between integrated spectra and CMD values as a function of cluster age (CMD value).

for which we present the following spectroscopic and photometric results.

(i) From the comparison of the cluster integrated spectrum with template cluster spectra, we found that the GGC template spectra G2 and G3 are the ones which best resemble the cluster integrated spectrum.

(ii) However, the extracted cluster CMD where its fiducial features are clearly seen reveals that Bruck 88 is a young cluster ($\log(t) = 8.1 \pm 0.1$). Note that the derived cluster age is compatible with the presence of a BRG star located ∼2.6 arcsec away from the direction towards the cluster centre. This result is opposite to that found from the cluster integrated spectrum, and makes us to wonder about the origin from which a young cluster appears much older to its integrated light.

(iii) We serendipitously observed HW 33 within the GMOS-S FOV, a star cluster located ≈3 arcmin (52.3 pc) to the south-east from Bruck 88. We obtained for the cluster the same $E(B - V)$ colour excess and age than Bruck 88 and surprisingly, a BRG star located within the cluster radius also appears to be compatible with the cluster age.

(iv) We estimated the MK type of the Bruck 88's BRG star to be in the range G9 II/Ib–K1 III. By combining the spectrum of a star within this MK type range with a 100–150 Myr template cluster integrated spectrum, we found that a proportion 85/15 in the sense BRG/template (BRG + template = 100) results in a spectrum which best resembles that of Bruck 88, independently of the BRG star LC. This result confirms that a BRG star dominates the cluster integrated spectrum, so that it causes the globular cluster appearance of its integrated light.

ACKNOWLEDGEMENTS

Based on observations obtained at the CTIO programme: 2003B-0447, which is operated by the Association of Universities for Research in Astronomy (AURA), Inc., under cooperative agreement with the NSF and at the Gemini Observatory (programme: GS-2013B-Q-60), which is operated by AURA, Inc., under a cooperative agreement with the NSF on behalf of the Gemini partnership: the National Science Foundation (United States), the Science and Technology Facilities Council (United Kingdom), the National Research Council (Canada), CONICYT (Chile), the Australian Research Council (Australia), Ministério da Ciência, Tecnologia e Inovação (Brazil) and Ministerio de Ciencia, Tecnología e Innovación Productiva (Argentina). I thank the astronomers at CTIO who carried out the observations. This research has made use of the SIMBAD data base, operated at CDS, Strasbourg, France, and draws upon data as distributed by the NOAO Science Archive. NOAO is operated by the Association of Universities for Research in Astronomy (AURA), Inc. under a cooperative agreement with the National Science Foundation. This work was partially supported by the Argentinian institutions CONICET and Agencia Nacional de Promoción Científica y Tecnológica (ANPCyT). I am grateful for the comments and suggestions raised by the anonymous referee which helped me to improve the manuscript.

REFERENCES

Ahumada A. V., Clariá J. J., Bica E., Piatti A. E., 2000, A&AS, 141, 79
Ahumada A. V., Clariá J. J., Bica E., Dutra C. M., Torres M. C., 2001, A&A, 377, 845
Ahumada A. V., Clariá J. J., Bica E., Dutra C. M., 2002, A&A, 393, 855
Ahumada A. V., Claria J. J., Bica E., Parisi M. C., Torres M. C., Pavani D. B., 2006, Bol. Asociacion Argentina Astron. La Plata Argentina, 49, 120
Ahumada A. V., Clariá J. J., Bica E., 2007, A&A, 473, 437
Ahumada A. V., Clariá J. J., Bica E., Parisi M. C., Palma T., 2008, Bol. Asociacion Argentina Astron. La Plata Argentina, 51, 69
Ahumada A. V., Clariá J. J., Bica E., 2009, Rev. Mex. Astron. Astrofis. Ser. Conf., 35, 156
Ahumada A. V., Benítez Llambay A., Santos J. F. C., Jr, Clariá J. J., Bica E., Piatti A. E., 2011, Rev. Mex. Astron. Astrofis. Ser. Conf., 40, 264
Asa'd R. S., Hanson M. M., Ahumada A. V., 2013, PASP, 125, 1304
Benítez-Llambay A., Piatti A. E., Clariá J. J., Palma T., Ahumada A. V., 2010, Bol Asociacion Argentina Astron. La Plata Argentina, 53, 161
Bica E., Alloin D., 1986a, A&AS, 66, 171
Bica E., Alloin D., 1986b, A&A, 162, 21
Bica E., Santiago B. X., Dutra C. M., Dottori H., de Oliveira M. R., Pavani D., 2001, A&A, 366, 827
Bica E., Bonatto C., Dutra C. M., Santos J. F. C., 2008, MNRAS, 389, 678
Bressan A., Marigo P., Girardi L., Salasnich B., Dal Cero C., Rubele S., Nanni A., 2012, MNRAS, 427, 127
Caldwell J. A. R., Cousins A. W. J., Ahlers C. C., van Wamelen P., Maritz E. J., 1993, SAAO Circ., 15, 1
Camargo D., Bonatto C., Bica E., 2009, A&A, 508, 211
Carraro G., Geisler D., Moitinho A., Baume G., Vázquez R. A., 2005, A&A, 442, 917
Carraro G., Beletsky Y., Marconi G., 2013, MNRAS, 428, 502
Chiosi E., Vallenari A., Held E. V., Rizzi L., Moretti A., 2006, A&A, 452, 179
Clariá J. J., Parisi M. C., Ahumada A. V., Santos J. F. C., Bica E., Piatti A. E., 2007, in Vazdekis A., Peletier R., eds, Proc. IAU Symp. 241, Stellar Populations as Building Blocks of Galaxies. Cambridge Univ. Press, Cambridge, p. 327
Crowl H. H., Sarajedini A., Piatti A. E., Geisler D., Bica E., Clariá J. J., Santos J. F. C., Jr, 2001, AJ, 122, 220
Da Costa G. S., Hatzidimitriou D., 1998, AJ, 115, 1934
Delgado A. J., Alfaro E. J., Yun J. L., 2011, A&A, 531, A141
Dias W. S., Alessi B. S., Moitinho A., Lépine J. R. D., 2002, A&A, 389, 871
Dieball A., Müller H., Grebel E. K., 2002, A&A, 391, 547
Dolphin A. E., Walker A. R., Hodge P. W., Mateo M., Olszewski E. W., Schommer R. A., Suntzeff N. B., 2001, ApJ, 562, 303
Dutra C. M., Bica E., Claria J. J., Piatti A. E., 1999, MNRAS, 305, 373
Glatt K., Grebel E. K., Koch A., 2010, A&A, 517, A50
Gouliermis D. A., Mackey D., Xin Y., Rochau B., 2010, ApJ, 709, 263
Jacoby G. H., Hunter D. A., Christian C. A., 1984, ApJS, 56, 257
Jones D. H. et al., 2009, MNRAS, 399, 683
Jordi K., Grebel E. K., Ammon K., 2006, A&A, 460, 339
Kerber L. O., Santiago B. X., Brocato E., 2007, A&A, 462, 139
Kharchenko N. V., Piskunov A. E., Röser S., Schilbach E., Scholz R.-D., 2005, A&A, 438, 1163
Kook S.-H., Sung H., Bessell M. S., 2010, J. Korean Astron. Soc., 43, 141
Lata S., Pandey A. K., Kumar B., Bhatt H., Pace G., Sharma S., 2010, AJ, 139, 378
Mackey A. D., Gilmore G. F., 2004, MNRAS, 352, 153
Maia F. F. S., Piatti A. E., Santos J. F. C., 2014, MNRAS, 437, 2005
Matteucci A., Ripepi V., Brocato E., Castellani V., 2002, A&A, 387, 861
Mighell K. J., Sarajedini A., French R. S., 1998, AJ, 116, 2395
Minniti J. H., Ahumada A. V., Clariá J. J., Benítez-Llambay A., Oddone M. A., Bica E., Santos J. F. C., Jr, 2012, Bol Asociacion Argentina Astron. La Plata Argentina, 55, 119
Minniti J. H., Ahumada A. V., Clariá J. J., Benítez-Llambay A., 2014, A&A, 565, A49
Moitinho A., Vázquez R. A., Carraro G., Baume G., Giorgi E. E., Lyra W., 2006, MNRAS, 368, L77
Mucciarelli A., Origlia L., Ferraro F. R., Maraston C., Testa V., 2006, ApJ, 646, 939
Oddone M. A., Palma T., Ahumada A. V., Clariá J. J., Bica E., Parisi M. C., Santos J. F. C., Jr, 2012, Bol Asociacion Argentina Astron. La Plata Argentina, 55, 131
Olsen K. A. G., Hodge P. W., Mateo M., Olszewski E. W., Schommer R. A., Suntzeff N. B., Walker A. R., 1998, MNRAS, 300, 665
Palma T., Ahumada A. V., Clariá J. J., Santos J. F. C., Jr, Bica E., 2008a, Acta Astron., 58, 359
Palma T., Ahumada A. V., Clariá J. J., Bica E., 2008b, Astron. Nachr., 329, 392
Pavani D. B., Kerber L. O., Bica E., Maciel W. J., 2011, MNRAS, 412, 1611
Perren G., Vázquez R. A., Carraro G., 2012, A&A, 548, A125
Piatti A. E., 2010, A&A, 513, L13
Piatti A. E., 2011, MNRAS, 416, L89
Piatti A. E., 2012, MNRAS, 422, 1109
Piatti A. E., 2014, MNRAS, 440, 3091
Piatti A. E., Clariá J. J., 2001, A&A, 370, 931
Piatti A. E., Geisler D., 2013, AJ, 145, 17
Piatti A. E., Sarajedini A., Geisler D., Bica E., Clariá J. J., 2002a, MNRAS, 329, 556
Piatti A. E., Bica E., Clariá J. J., Santos J. F. C., Ahumada A. V., 2002b, MNRAS, 335, 233
Piatti A. E., Bica E., Santos J. F. C., Jr, Clariá J. J., 2002c, A&A, 387, 108
Piatti A. E., Geisler D., Bica E., Clariá J. J., 2003a, MNRAS, 343, 851
Piatti A. E., Bica E., Geisler D., Clariá J. J., 2003b, MNRAS, 344, 965

Piatti A. E., Sarajedini A., Geisler D., Seguel J., Clark D., 2005a, MNRAS, 358, 1215
Piatti A. E., Santos J. F. C., Jr, Clariá J. J., Bica E., Ahumada A. V., Parisi M. C., 2005b, A&A, 440, 111
Piatti A. E., Clariá J. J., Ahumada A. V., 2006, New Astron., 11, 262
Piatti A. E., Sarajedini A., Geisler D., Gallart C., Wischnjewsky M., 2007a, MNRAS, 381, L84
Piatti A. E., Sarajedini A., Geisler D., Gallart C., Wischnjewsky M., 2007b, MNRAS, 382, 1203
Piatti A. E., Clariá J. J., Ahumada A. V., 2009, MNRAS, 397, 1073
Piatti A. E., Clariá J. J., Ahumada A. V., 2010a, PASP, 122, 516
Piatti A. E., Clariá J. J., Ahumada A. V., 2010b, MNRAS, 408, 1147
Piatti A. E., Clariá J. J., Ahumada A. V., 2011a, New Astron., 16, 161
Piatti A. E., Clariá J. J., Bica E., Geisler D., Ahumada A. V., Girardi L., 2011b, MNRAS, 417, 1559
Piatti A. E., Keller S. C., Mackey A. D., Da Costa G. S., 2014, MNRAS, 444, 1425
Rose J. A., 1984, AJ, 89, 1238
Rose J. A., 1985, AJ, 90, 1927
Santos J. F. C., Jr Alloin D., Bica E., Bonatto C. J., 2002, in Geisler D. P., Grebel E. K., Minniti D., eds, Proc. IAU Symp. 207, Extragalactic Star Clusters. Astron. Soc. Pac., San Francisco, p. 727
Santos J. F. C., Jr, Piatti A. E., 2004, A&A, 428, 79 (SP04)
Santos J. F. C., Jr, Clariá J. J., Ahumada A. V., Bica E., Piatti A. E., Parisi M. C., 2006, A&A, 448, 1023
Santos-Silva T., Gregorio-Hetem J., 2012, A&A, 547, A107
Schmidt-Kaler T., 1982, Landolt-Börnstein: Numerical Data and Functional Relationships in Science and Technology, New Series, Group VI, Vol. 2b. Springer-Verlag, Berlin
Schuster W. J., Moitinho A., Márquez A., Parrao L., Covarrubias E., 2006, A&A, 445, 939
Stetson P. B., Davis L. E., Crabtree D. R., 1990, in Jacoby G. H., ed., ASP Conf. Ser. Vol. 8, CCDs in Astronomy. Astron. Soc. Pac., San Francisco. p. 289
Stone R. P. S., Baldwin J. A., 1983, MNRAS, 204, 347
Talavera M. L., Ahumada A. V., Clariá J. J., Santos J. F. C., Bica E., Torres M. C., Jr, 2007, Bol. Asociacion Argentina Astron. La Plata Argentina, 50, 157
Talavera M. L., Ahumada A. V., Clariá J. J., Santos J. F. C., Jr, Bica E., Parisi M. C., 2009, Rev. Mex. Astron. Astrofis. Ser. Conf., 35, 117
Talavera M. L., Ahumada A. V., Santos J. F. C., Jr, Clariá J. J., Bica E., Parisi M. C., Torres M. C., 2010, Astron. Nachr., 331, 323
Tapia M. T., Schuster W. J., Michel R. C., Chavarrí a-K., Dias W. S., Vázquez R., Moitinho A., 2010, MNRAS, 401, 621
Vázquez R. A., May J., Carraro G., Bronfman L., Moitinho A., Baume G., 2008, ApJ, 672, 930
Vázquez R. A., Moitinho A., Carraro G., Dias W. S., 2010, A&A, 511, A38

SUPPORTING INFORMATION

Additional Supporting Information may be found in the online version of this article:

Table 2. CCD *gi* data of stars in the field of Bruck 88 (http://mnras.oxfordjournals.org/lookup/suppl/doi:10.1093/mnras/stu1917/-/DC1).

Please note: Oxford University Press is not responsible for the content or functionality of any supporting materials supplied by the authors. Any queries (other than missing material) should be directed to the corresponding author for the paper.

This paper has been typeset from a TEX/LATEX file prepared by the author.